COLO HEP 413

Study of Point 1 Supersymmetric Neutralinos: $\widetilde{\chi}_1^0$ and $\widetilde{\chi}_2^0$ in a 60% Left Polarized Beam

Deborah L. Weber

December 30, 1998

COLO HEP 413

Abstract

Supersymmetry is a theory that may solve the deficiencies of the Standard Model of elementary particle interactions. This report details the search for two Supersymmetric Particles, namely the $\widetilde{\chi}_1^0$ and the $\widetilde{\chi}_2^0$, which occur as a result of the reaction $\mathrm{e}^+ + \mathrm{e}^- \rightarrow \widetilde{\chi}_1^0 + \widetilde{\chi}_2^0$. The search was performed using computer simulations of Supersymmetric parameters decided upon at the Snowmass '96 conference, using the mSUGRA model. The study described by this report shows how these Supersymmetric particles' decays may be detected in an e^+e^- collider at 500 GeV with a 60% left polarized electron beam.

Contents

List of Tables

List of Figures

1 Introduction

My research took place in the field of elementary particle physics/high energy physics. Elementary particle physics is the study of the fundamental particles that make up matter. These particles are called “fundamental” because we believe, at the present time, that they cannot be broken down into smaller particles. In high energy physics we study the interaction of these elementary particles in the hope to uncover how the world in which we live was formed. We have learned in the last hundred years that this picture seems to become clearer when we study these interactions at ever higher energies.

The Standard Model of elementary particle interactions states that all matter is made up of two groups of fundamental particles called quarks and leptons. Table 1 shows a listing of quarks and leptons. The top quark, the heaviest member of this table, was discovered in 1995. It may be observed that there are an equal number of quarks and leptons, namely six. The reason for this number is not understood at this time.

Table 1: Listing of Quarks and Leptons

Particle	Name	Symbol	Particle	Name	Symbol
Quarks	up	u	Leptons	electron	e
	down	d		electron neutrino	ν_e
	charm	c		muon	μ
	strange	s		muon neutrino	ν_μ
	top	t		tau	τ
	bottom	b		tau neutrino	ν_τ

The Standard Model also states that there are three different interactions: strong, weak, and electromagnetic[1]. A list of the interactions and their mediators can be seen in Table 2. The only carrier shown in the table that has never been observed is the graviton. The gravitational interaction is a fourth interaction which is not part of the Standard Model. To date, we have not been able to discover as much about the gravitational interaction as we have about the other three.

[1]the weak and electromagnetic interactions have been combined into one interaction: the *electroweak* interaction.

Table 2: Listing of Interactions [1, pp. 19-20]

Interaction	Carrier	Symbol	Spin	Characteristic
Gravitational	graviton		2	Acts between all particles with mass
Electromagnetic	photon	γ	1	Acts between all electrically charged particles
Strong	gluon	g	1	Acts between quarks and is responsible for holding the nucleus together
Weak	W, Z boson	W^+, W^-, W^0, Z^0	1	Acts between quarks & quarks, quarks & leptons, and leptons & leptons; responsible for radioactivity

In the Standard Model, we must add a new field, called the Higgs field. The Higgs field introduces a particle called the Higgs boson. Without Higgs bosons, the particles do not have mass. The Standard Model describes massless particles. This is due to the fact that adding the diagrams of all interactions leads to infinities because of ambiguities in defining the electron and the photon [2, p. 31]. See Figure 1 for diagrams that give samples of the infinite contributions when added together. The Standard Model theory is finite (in

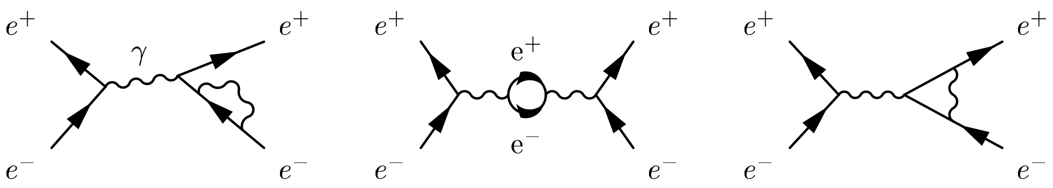

Figure 1: Diagrams with "bubbles" which give infinite contributions [2, p. 31].

the same sense that electromagnetism is finite) only with the inclusion of the Higgs particle [3, p. 255]. The Standard Model particles do not have mass without the inclusion of the Higgs field.

Because of the ambiguities and the infinities they cause, we must use the process of renormalization. According to J. E. Dodd, renormalization "is a necessary formal process which shows that the particles in the theory and their interactions are consistent with the principles of quantum theory" [2, p. 31]. However, the renormalization process causes the Higgs mass to become infinite, which is a property of a spin-0 particle. This divergence of the Higgs mass is one of the inadequacies of the Standard Model.

Although the Standard Model is very good at explaining all of low energy interactions, physicists know that the Standard Model is not perfect. The inadequacies of the Standard Model are that it leads to an infinite Higgs mass, the coupling constants of the three interactions do not extrapolate to a single value at high energies, and it requires many arbitrary parameters [4, p. 80]. Supersymmetry is one theory which corrects the inadequacies of the Standard Model. It may even give us a better understanding of the gravitational interaction, although this idea is very tenuous. The introduction of Supersymmetric particles to the Standard Model seems to unify the three better-known interactions' couplings into one coupling at very high energies, on the order of 10^{14} GeV, and, therefore, quite possibly cause a unification of these three interactions.

In certain interactions called annihilations, two particles collide in such a way that they disappear completely (that is, they annihilate each other). The annihilations create a large amount of energy. This energy can be used to form new particles. Some of these particles, like the ones that I am studying, decay very rapidly. Many theoretical physicists believe that these annihilations can create supersymmetric particles. No one has been able to observe these particles. As yet, they are still merely theoretical. My research is helping to design a detector to see supersymmetric particles, if they exist.

2 Background Information

Supersymmetry theory states that for every fundamental particle, there is a supersymmetric partner. The supersymmetric particles are named very similarly to their Standard Model partners. For fermions, such as quarks and leptons, the supersymmetric partners are named by adding an s to the front of the Standard Model particle, for instance: *squarks* and *sleptons*. Thus, the supersymmetric partner to an up quark is an up $s$quark, the supersymmetric partner to an electron is a $s$electron, and so on. For bosons, the supersymmetric partners are named by adding the ending -*ino* to the name of the Standard Model boson. For instance, the supersymmetric partner to a photon is a phot*ino* and the supersymmetric partner to a W-boson is a W*ino*. The symbols for supersymmetric particles are nearly the same; a tilde ($\tilde{}$) is added above the symbol. Hence, the up squark would be denoted by $\widetilde{u}$, the selectron by $\widetilde{e}^-$, the photino by $\widetilde{\gamma}$, and the Wino by $\widetilde{W}$.

Each supersymmetric particle is equal in charge and differs in spin by $\frac{1}{2}\hbar$ from its Standard Model partner, where $\hbar = \frac{h}{2\pi}$ ($h = 4.14 \times 10^{-15} eV \cdot sec$—Planck's Constant). Spin is an important property; it is quantized and measured in multiples of $\hbar$. A particle whose spin, n, is a half-integer is a fermion, and one whose spin is an integer is a boson. The Higgs boson, which has never been experimentally observed, has a spin of 0. The Supersymmetric fermions have integer spins and the Supersymmetric bosons have half-integer spins. Fermions are particles that make up matter in the world around us. They consist of quarks and leptons, as are shown in Table 1. Bosons are carriers of the four interactions, shown in Table 2.

Theorists surmise that there must be supersymmetric particles in our world. This is due to the fact that although the Standard Model describes the low energy world with great accuracy, it runs into problems at high energies. The Standard Model is incomplete. Eventually, at some energy scale, its interactions become strong. This phenomenon suggests that there is a better, more complete model of matter, which exists at higher energies and of which the Standard Model is a part. The deficiencies, as stated earlier, are that the coupling constants of the three Standard Model interactions do not meet at high energies and that the Higgs mass diverges. Supersymmetry theory holds that, at some high energy, the coupling constants of the three interactions will meet, with Supersymmetry acting as an agent facilitating that unification. The addition of Supersymmetric sparticles (those that partner the Standard Model particles) to the Standard Model causes the infinite terms of the Higgs mass to cancel, thereby giving the Higgs particle a finite mass.

In Supersymmetry theory, there is a Z_2 symmetry called R-parity. R-parity conservation forbids squark-mediated weak-scale proton decay. For ordinary particles, R-parity is defined to be +1. For their supersymmetric partners, the R-parity is –1. R-parity conservation holds that supersymmetric particles are produced in pairs by collisions of ordinary particles and that they decay into other supersymmetric particles, finally decaying to the Lightest Supersymmetric Particle (LSP) and other particles. Additionally, R-parity implies that the LSP is stable. The LSP is assumed to be the $\widetilde{\chi}_1^0$ particle, which is the lightest neutralino. $\widetilde{\chi}_1^0$ does not decay and is not experimentally detectable. Since it is not detectable and is the particle into which all supersymmetric particles eventually decay, if R-parity is conserved, a characteristic of supersymmetry is a large amount of missing energy and momentum [5, p. 643].

In 1996, high energy physicists held a conference at Snowmass, Colorado, where they considered diverse models of supersymmetry. At that conference, they chose a minimal Supergravity Model, called mSUGRA. The attractiveness of this model is that there is one common Supersymmetry-breaking scalar mass parameter, m_0, one bilinear scalar coupling, B_0, and one trilinear scalar coupling, A_0. There is also a universal gaugino mass, $m_{\frac{1}{2}}$ (which comes from the assumption of an underlying grand unification). Therefore, the model is specified completely by the parameters μ (μ denotes the supersymmetric Higgs mass term), m_0, $m_{\frac{1}{2}}$, A_0, and B_0. The parameter B_0 was replaced by $tan\beta$, where $tan\beta = \frac{v_u}{v_d}$, the ratio of up- to down-type vacuum expectation values [5, pp. 644-645]. Table 3 shows the parameters of the five points.

Table 3: List of values for the five parameter sets, as specified by the Snowmass '96 Conference. *NOTE: Point 4 is the only non-SUGRA-inspired point.*

Parameter	Point 1	Point 2	Point 3	Point 4	Point 5
m_0	400	100	200	—	300
$m_{\frac{1}{2}}$	200	300	100	—	150
A_0	0	0	0	—	-600
$tan\beta$	2	2	2	10	2
μ	-490	-534	-253	-100	444

Table 4 shows the mass spectrum of the Supersymmetric particles based on the parameters in Table 3.

Table 4: Mass Spectrum (in GeV) of the Five Supersymmetric Points

	Point 1	Point 2	Point 3	Point 4	Point 5
$\widetilde{\chi}_1^0$	86.05	128.70	44.52	77.83	57.17
$\widetilde{\chi}_2^0$	175.45	257.22	97.00	115.29	111.46
$\widetilde{\chi}_3^0$	492.70	535.50	256.94	146.84	444.77
$\widetilde{\chi}_4^0$	501.75	542.54	273.64	292.41	464.60
$\widetilde{\chi}_1^\pm$	175.34	257.20	96.39	96.06	110.10
$\widetilde{\chi}_2^\pm$	500.81	542.24	272.04	292.46	461.60
h^0	83.25	89.92	68.29	126.96	101.42
H^0	745.30	681.40	378.99	201.61	622.61
A^0	741.05	676.41	371.09	200.00	620.01
$H^\pm$	744.61	680.33	378.49	214.81	624.10
$\widetilde{\nu}_\ell$	421.40	230.02	206.62	1000.00	314.60
$\widetilde{e}_L^\pm$	425.92	238.21	215.70	1000.00	320.64
$\widetilde{e}_R^\pm$	408.80	156.95	206.62	1000.00	307.45
$\widetilde{t}_1$	424.43	535.82	263.71	924.84	150.66
$\widetilde{b}_L$	520.57	621.86	274.27	1000.00	380.76
$\widetilde{q}_L$	603.27	668.38	316.73	1000.00	462.49
$\widetilde{t}_2$	550.61	656.48	329.48	1096.29	494.73
$\widetilde{b}_R$	595.55	653.10	312.97	1000.00	456.58
$\widetilde{q}_R$	603.27	668.38	316.73	1000.00	462.49
$\widetilde{g}$	550.62	759.04	298.40	900.00	425.52

3 Methods Used in the Study

The point that I studied was Point 1. In particular, I was trying to "experimentally" determine the masses of the $\widetilde{\chi}_1^0$ and $\widetilde{\chi}_2^0$. The "experiment" was performed by using computer simulations of the production of these supersymmetric particles and then analyzing the observed particles resulting from their decays to see whether we could determine the masses of the initial states, which are the $\widetilde{\chi}_1^0$ and $\widetilde{\chi}_2^0$.

The procedure that I followed this summer is as follows:

- Perform computer simulations of the reaction $\mathrm{e}^+ + \mathrm{e}^- \to \widetilde{\chi}_1^0 + \widetilde{\chi}_2^0$. At 500 GeV, the cross section for a 60% left polarized electron beam is predicted to be 44 fb, and for 60% right polarized electron beam is predicted to be 10 fb. See Table 5 for the cross sections of the production of the various supersymmetric particles.

Table 5: Cross Sections (in fb) for Various Point 1 Production Modes

	350 GeV		500 GeV		1000 GeV		1500 GeV	
	60% L	60% R	60% L	60% R	60% L	60% R	60% L	60% R
$\widetilde{\chi}_1^0\widetilde{\chi}_1^0$	28	88	40	122	32	96	20	59
$\widetilde{\chi}_2^0\widetilde{\chi}_2^0$			32	8	50	12	34	8
$\widetilde{\chi}_1^0\widetilde{\chi}_2^0$	18	4	44	10	41	10	28	8
$\widetilde{\chi}_3^0\widetilde{\chi}_4^0$					8	6	21	18
$\widetilde{\chi}_1^+\widetilde{\chi}_1^-$			527	132	171	44	102	26
$\widetilde{\chi}_2^+\widetilde{\chi}_2^-$							68	29
$h^0 Z^0$	174	144	69	58	15	12	6	6
$\widetilde{\nu}_e\widetilde{\nu}_e$					227	58	445	113
$\widetilde{e}_L^+\widetilde{e}_L^-$					47	13	122	32
$\widetilde{e}_R^+\widetilde{e}_R^-$					19	69	38	143
$\widetilde{t}_1\widetilde{t}_1$					3	7	6	11
total	220	236	712	330	613	327	890	453

- Separate the $\widetilde{\chi}_1^0\widetilde{\chi}_2^0$ signal from other Supersymmetric production modes by applying cuts that leave as much as possible of $\widetilde{\chi}_1^0\widetilde{\chi}_2^0$.

- Plot the reconstructed mass of the jets into which the Higgs particle (a decay product of the $\widetilde{\chi}_2^0$) decays in order to find the mass of the Higgs.

The mass of the Higgs is required to find the masses of the $\widetilde{\chi}_1^0$ and $\widetilde{\chi}_2^0$ particles.

- Plot a histogram of the visible energy of the particle jets that survived the cuts.

- Perform a box fit of the visible energy histogram. We perform a box fit because we need to have a low energy endpoint (designated as minimum energy, or E_{min}), a high energy endpoint (designated as maximum energy, or E_{max}), and a flat distribution.

- Use the center of mass energy (E_{cm}) as well as E_{min} and E_{max} (the endpoints found in the previous step) to determine the mass of the $\widetilde{\chi}_1^0$ and the mass of the $\widetilde{\chi}_2^0$.

4 Analysis

In order to perform the simulations of Point 1 parameters, I used a program called *ISAJET*. In the parameter file, I was required to stipulate the center of mass energy (E_{cm}), the number of events, and the polarization of the electron-positron beam. The polarization of the beam is an important part of the initial conditions. The polarization of the beam allows us to vary the strength of the signal and the background. For instance, at 500 GeV, a 60% left polarized beam is predicted to produce the $\widetilde{\chi}_1^0\widetilde{\chi}_2^0$ signal at a cross section of 44 fb, which is much larger than the $\widetilde{\chi}_1^0\widetilde{\chi}_2^0$ signal that is predicted to be produced from a 60% right polarized beam. Additionally, the background can be decreased in this way as well. For example, the $\widetilde{\chi}_1^0\widetilde{\chi}_1^0$ signal is three times larger at 60% right polarized than it is at 60% left polarized. Although the $\widetilde{\chi}_1^0\widetilde{\chi}_1^0$ signal doesn't make a great deal of difference, since the $\widetilde{\chi}_1^0$ has no visible energy, the example illustrates the concept, which is helpful at other points (such as Point 3). Therefore, in my case, I used a 60% left polarized beam in order to increase the cross section of the $\widetilde{\chi}_1^0\widetilde{\chi}_2^0$ signal.

To maximize the signal's cross section further, I chose the center of mass energy (E_{cm}) to be 500 GeV. 500 GeV is where we expect to start searching for Supersymmetric phenomena. Note from Table 5 that at this E_{cm} the $\widetilde{\chi}_1^+\widetilde{\chi}_1^-$ is at a large cross section, approximately 12 times the cross section of the $\widetilde{\chi}_1^0\widetilde{\chi}_2^0$ signal's cross section. Unfortunately, this observation shows that the $\widetilde{\chi}_1^+\widetilde{\chi}_1^-$ signal is the major Supersymmetric background in my study.

To calculate the number of events to run (an event is the same thing as an interaction or annihilation), I had to calculate the number of events that would occur in one "year" of data collection. One "year" of running is not the same as one calendar year; it is 10^7 seconds. That is about 116 days of data collection (just under 4 months). To get this figure, I took the total cross-section (in fb) at 500 GeV, left polarized and multiplied it by 50 fb^{-1}. 50 fb^{-1} is the yearly luminosity of the accelerator, which, when multiplied by the cross-section, will give the number of particles produced in that amount of time (namely, one "year").

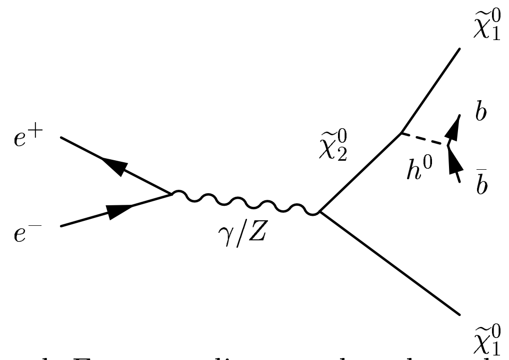

Figure 2: $\widetilde{\chi}_1^0$ $\widetilde{\chi}_2^0$ Signal. Feynman diagram that shows how the $\widetilde{\chi}_1^0\widetilde{\chi}_2^0$ signal is produced and how it decays given the mSUGRA parameters of Point 1.

Figure 2 shows the Feynman diagram depicting the process by which the $\widetilde{\chi}_1^0\widetilde{\chi}_2^0$ signal is produced and how it decays given the mSUGRA parameters of Point 1. There are three other possibilities of observing the $\widetilde{\chi}_1^0\widetilde{\chi}_2^0$ decay, based upon the branching ratios of the Higgs particle. A branching ratio describes the probability that a particular particle will decay in a particular way. The $\widetilde{\chi}_2^0 \to \widetilde{\chi}_1^0 + h^0$ decay occurs at a branching ratio of 99.6%. Figure 2 shows the case where the Higgs decays into a $b\bar{b}$, which represents a branching ratio of 88.7% for the Higgs particle; the other three signals have branching ratios of 5.0% or less. Note that the Higgs decay I used is $h^0 \to b + \bar{b}$. The remaining three Higgs decays are as follows:

$$\begin{array}{ll} h^0 \to c + \bar{c} & (4.3\%) \\ h^0 \to \tau^- + \tau^+ & (5.0\%) \\ h^0 \to g + g & (1.6\%) \end{array}$$

From Table 5, one can see that at 500 GeV, there would be four other signals produced. These signals are $\widetilde{\chi}_1^0\widetilde{\chi}_1^0$, $\widetilde{\chi}_2^0\widetilde{\chi}_2^0$, $\widetilde{\chi}_1^+\widetilde{\chi}_1^-$, and h^0Z^0. The most abundant signal at 500 GeV is the $\widetilde{\chi}_1^+\widetilde{\chi}_1^-$ signal, with a cross section of 527 fb for 60% left polarized and 132 fb at 60% right polarized.

4.1 The Cuts

The cuts that I made to enhance the $\widetilde{\chi}_1^0\widetilde{\chi}_2^0$ signal over the background are as follows:

- Cut 1: Require all events to have visible energy
- Cut 2: Require all events to have more than three visible particles
- Cut 3: Require all events to have less than 50 GeV of energy in the backward direction (E_{back})
- Cut 4: Require all events to have less than 200 GeV of energy difference between E_{for} (energy in the forward direction) and E_{back}
- Cut 5: Require all events to contain no e^+, e^-, μ^+, μ^-
- Cut 6: Require all events to have two b-quark jets

Table 6 shows the effect of the cuts on my signal. The computer simulations were able to identify the particles, but we cannot identify them outside of computer simulations, since that is the purpose of building the detector. The following table is based on the assumption that the $\widetilde{\chi}_1^0$ and $\widetilde{\chi}_2^0$ particles were able to be identified by the computer.

Table 7 shows the effectiveness of the cuts on the various supersymmetric backgrounds as well as the $h^0 Z^0$ background. As with Table 6, the identification of the particles is not as easily done as asking the computer to separate certain particles with certain IDs from the signal for which I am looking.

Table 6: Effect of Cuts on My Signal.

Cut	Number of Events Remaining	Percentage of Signal Remaining From	
		Previous Cut	Initial Signal Strength
Uncut	2130	Not Applicable	Not Applicable
Cut 1	2130	100%	100%
Cut 2	2097	98.5%	98.5%
Cut 3	2095	99.9%	98.4%
Cut 4	2095	100%	98.4%
Cut 5	793	37.9%	37.2%
Cut 6	635	81.1%	29.8%

Table 7: Effectiveness of Cuts on Supersymmetric Background. Note that this table refers to the background reduction, not to the remaining background.

Signal	Cut	Number of Events Remaining	Percentage of Signal Reduction From Previous Cut	Percentage of Signal Reduction From Initial Signal Strength
$\widetilde{\chi}_2^0\widetilde{\chi}_2^0$	Uncut	1645	Not Applicable	Not Applicable
	Cut 1	1645	0%	0%
	Cut 2	1645	0%	0%
	Cut 3	80	95.1%	95.1%
	Cut 4	80	0%	95.1%
	Cut 5	8	90.0%	99.5%
	Cut 6	7	12.5%	99.6%
$\widetilde{\chi}_1^+\widetilde{\chi}_1^-$	Uncut	25626	Not Applicable	Not Applicable
	Cut 1	25626	0%	0%
	Cut 2	23552	8.1%	8.1%
	Cut 3	5780	75.5%	77.4%
	Cut 4	5780	0%	77.4%
	Cut 5	1354	76.6%	94.7%
	Cut 6	60	95.6%	99.8%
h^0Z^0	Uncut	3579	Not Applicable	Not Applicable
	Cut 1	3579	0%	0%
	Cut 2	3570	0.3%	0.3%
	Cut 3	728	79.6%	79.7%
	Cut 4	124	83.0%	96.5%
	Cut 5	20	83.9%	99.4%
	Cut 6	4	80.0%	99.9%

4.1.1 Cut 1

The first signal, $\widetilde{\chi}_1^0\widetilde{\chi}_1^0$, consists entirely of the Lightest Supersymmetric Particle (LSP). Recall from earlier that the LSP is experimentally undetectable. That is, $\widetilde{\chi}_1^0$ has no visible energy. Eliminating this part of the background was a simple cut of requiring that all events had visible energy. This cut was necessary for a computer simulation but completely superfluous for an actual experiment, as our instruments will only be capable of measuring visible energy.

4.1.2 Cut 2

The second cut that I made required each event to have more than three visible particles. The reason I chose this cut was that when the Higgs particle in my signal decays into $b\bar{b}$ jets, the jets produce many more than three visible particles. Although this cut did not affect my supersymmetric background very much, it may have a large impact on the Standard Model Background which will be added later.

4.1.3 Cut 3

The third cut I made was to remove any events whose energy in the backward direction (E_{back}) was greater than 50 GeV. To understand E_{back} and E_{for} (the energy in the forward direction), one must understand a little about how each interaction takes place. In the case of the reaction $e^+ + e^- \rightarrow \widetilde{\chi}_1^0 + \widetilde{\chi}_2^0$, two particles will be created from the annihilation: $\widetilde{\chi}_1^0$ and $\widetilde{\chi}_2^0$. The $\widetilde{\chi}_1^0$ and the $\widetilde{\chi}_2^0$ will move away, back to back, from the annihilation's center. The thrust axis is the line upon which the majority of the momentum of the $\widetilde{\chi}_1^0$ and $\widetilde{\chi}_2^0$ lies. A plane that lies perpendicular to the thrust axis is the line which separates the energy in the forward direction (E_{for}) from the energy in the backward direction (E_{back}). The forward direction is defined as the hemisphere which has the higher amount of energy and the backward direction is defined as the hemisphere which has the lower amount of energy.

Because the $\widetilde{\chi}_1^0\widetilde{\chi}_2^0$ signal is quite asymmetrical (note Figure 3), the energy in the backward direction should be quite low. One would almost expect E_{back} to be zero. However, this is not the case since there can be energy from one of the b-quark jets straying over the E_{for}/E_{back} boundary.

I chose 50 GeV to be my defining backward energy because I retain a clear low energy edge and a flat distribution when I require events to have

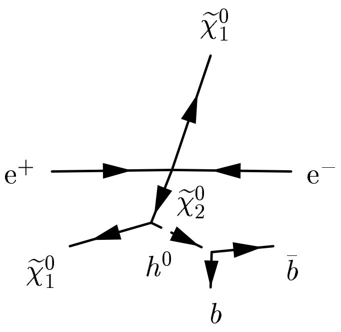

Figure 3: Diagram illustrating asymmetry of $\widetilde{\chi}_1^0\widetilde{\chi}_2^0$ signal.

an E_{back} less than 50 GeV. Requiring the cut at a lower E_{back} made the low energy edge of the Higgs particle less distinct and changed the distribution of the signal so that it was no longer flat. Notice Figure 4.

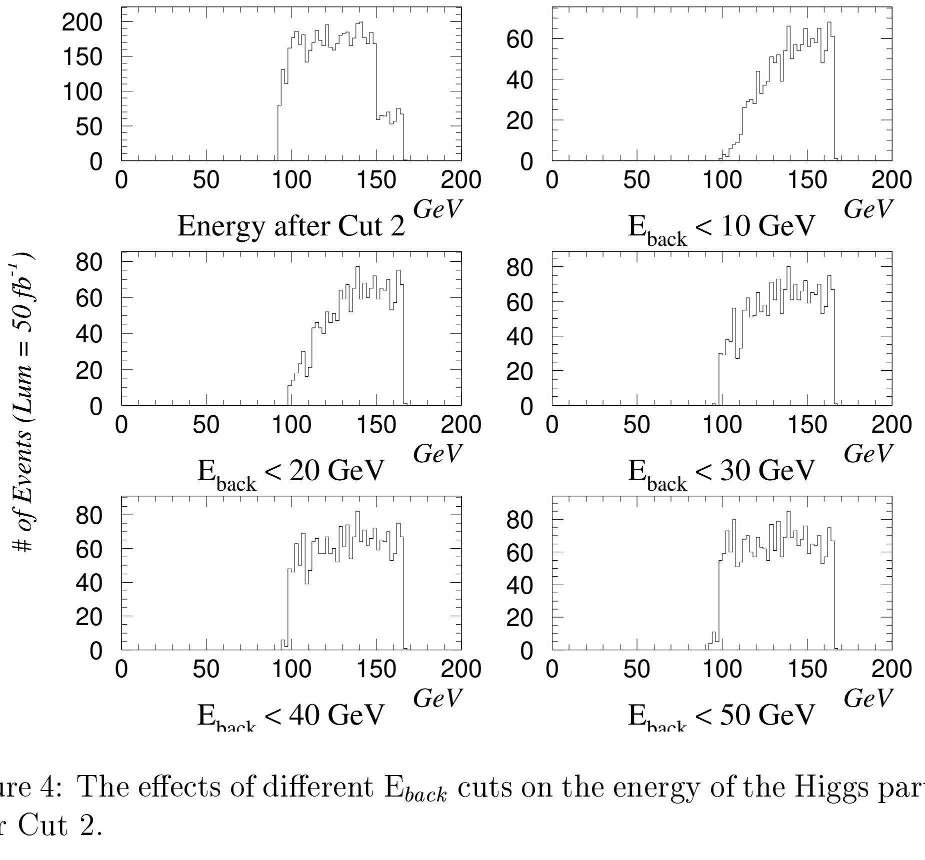

Figure 4: The effects of different E_{back} cuts on the energy of the Higgs particle after Cut 2.

This cut reduced the $\widetilde{\chi}_2^0\widetilde{\chi}_2^0$ signal significantly (as shown in Table 7). The reduction of $\widetilde{\chi}_2^0\widetilde{\chi}_2^0$ is due to the fact that the $\widetilde{\chi}_2^0\widetilde{\chi}_2^0$ signal is very symmetric, as one can see from Figure 5.

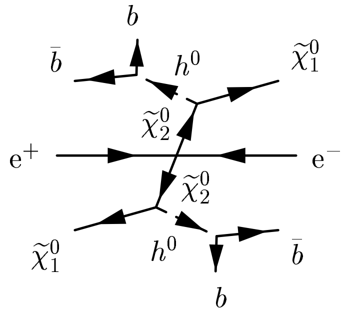

Figure 5: Diagram illustrating symmetry of $\widetilde{\chi}_2^0\widetilde{\chi}_2^0$ signal.

This cut also reduced the h^0Z^0 signal, as one can see from Table 7. In particular, it removed a visible energy (E_{vis}) peak near 500 GeV. Figure 6 shows the peak at 500 GeV. This peak is due to the fact that the h^0Z^0

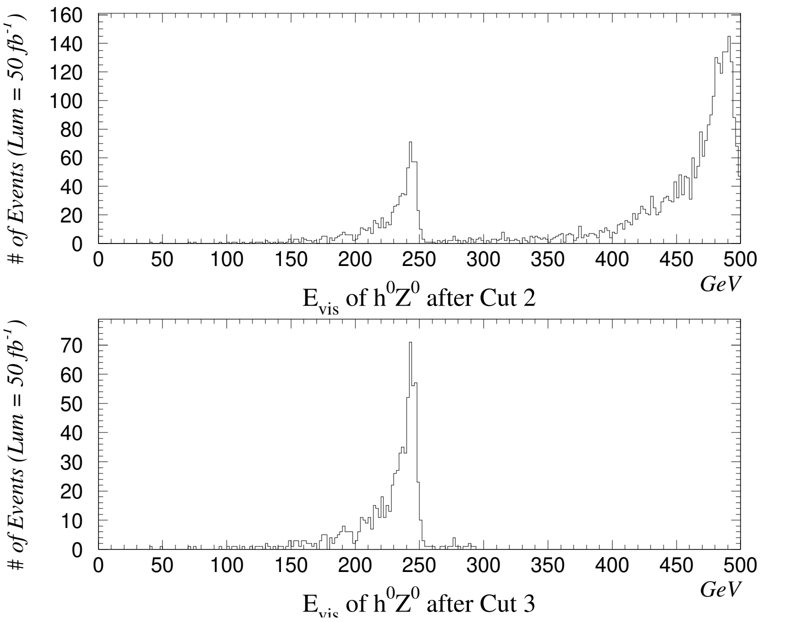

Figure 6: Set of plots showing the visible energy of the h^0Z^0 signal. Top plot shows E_{vis} before Cut 3 and bottom plot shows E_{vis} after Cut 3.

signal decays entirely into visible particles, as shown in Figure 7. Each of

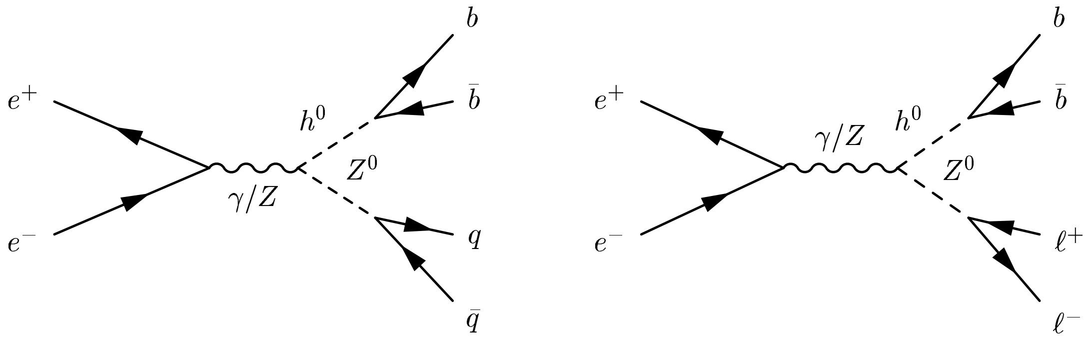

Figure 7: Feynman diagrams depicting two processes by which the h^0Z^0 signal can be produced. Note the branching for the left signal is 62.0% and the branching ratio for the right signal is 3.0%.

these particle decays will have visible energy on both sides of the $\mathrm{E}_{for}/\mathrm{E}_{back}$ boundary.

4.1.4 Cut 4

In the fourth cut, I required $\mathrm{E}_{for} - \mathrm{E}_{back}$ to be less than 200 GeV. This cut, as shown by Table 7, reduced the h^0Z^0 signal further. Although the previous cut removed the E_{vis} peak near 500 GeV, there remained a peak near 250 GeV, as shown in Figure 8. This peak is due to the fact that, in addition to the decays shown in Figure 7, the h^0Z^0 can also decay as shown in Figure 9. This figure shows the Z^0 decaying into neutrinos, which are invisible. Therefore, the signal appears asymmetrical, with very little energy in the backward direction and it passes Cut 3.

With little if any visible energy in the backward direction and nothing but visible energy in the forward direction, the difference between E_{for} and E_{back} should be close to 250 GeV for the h^0Z^0 signal. This is because the mass of the Higgs particle is predicted to be close to that of the Z^0 particle (compare 83.25 GeV for the h^0 to 91.19 GeV for the Z^0). With a center of mass energy (E_{cm}) of 500 GeV, each particle coming away from the interaction should have a momentum of approximately 250 GeV. Since the Z^0 decays into neutrinos,

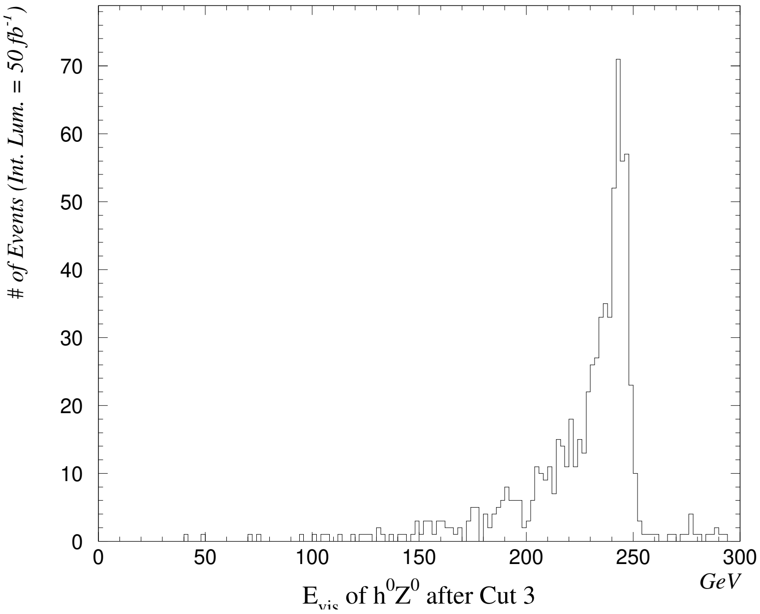

Figure 8: Visible Energy of h^0Z^0 signal after Cut 3.

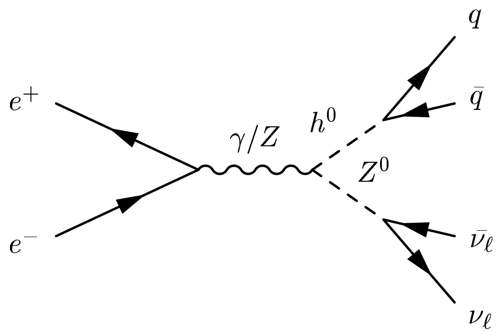

Figure 9: Feynman diagram depicting another of the processes by which the h^0Z^0 signal is produced. Note that the branching ratio for this particular decay is 17.7%.

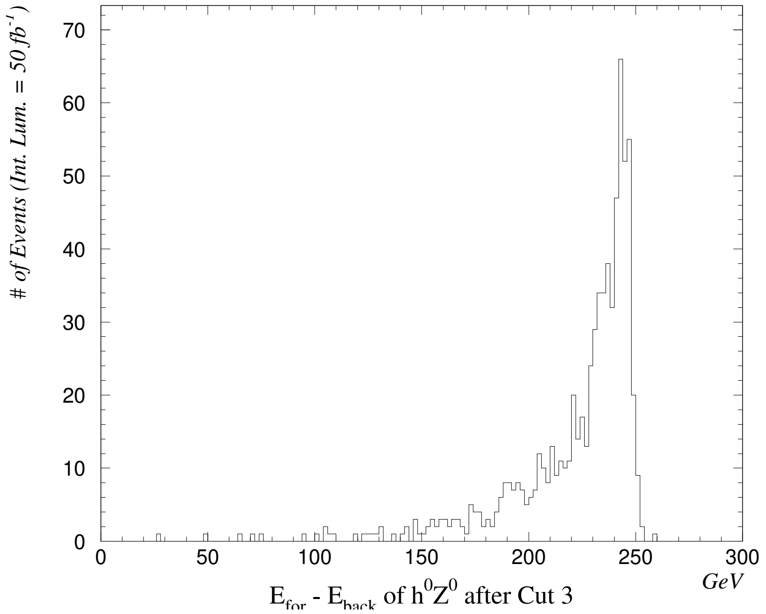

Figure 10: E_{for} - E_{back} of h^0Z^0 signal after Cut 3.

which are invisible, the difference between E_{for} and E_{back} should be close to 250 GeV. This difference is illustrated by the plot shown in Figure 10.

Notice from Table 6 that Cut 4 does not affect the $\widetilde{\chi}_1^0\widetilde{\chi}_2^0$ signal at all. This is due to the fact that $\widetilde{\chi}_1^0\widetilde{\chi}_2^0$, as a supersymmetric signal, has missing energy. The $\widetilde{\chi}_1^0$ particle, in this case, is similar to the Z^0 in that the decay of the Z^0 is invisible (since the decay products are neutrinos). Since the Z^0 is detected by its decay products, one could say, that, in this case, the Z^0 behaves in a manner similar to the $\widetilde{\chi}_1^0$. The $\widetilde{\chi}_2^0$ particle, in this case (and all others) is not similar to the h^0 particle. Recall that the $\widetilde{\chi}_2^0$ decays into a $\widetilde{\chi}_1^0$ and a h^0. Since the $\widetilde{\chi}_1^0$ is not detectable, the $\widetilde{\chi}_2^0$ decay has missing energy where the h^0 decay does not. Thus, while the h^0Z^0 signal has no missing energy in the forward direction, the $\widetilde{\chi}_1^0\widetilde{\chi}_2^0$ signal has missing energy in the forward direction. Note Figure 11, which shows that the difference between E_{for} and E_{back} for the $\widetilde{\chi}_1^0\widetilde{\chi}_2^0$ signal is less than 200 GeV. However, I cannot make a cut based solely upon Figure 11, since it shows the particles for which I'm looking. In a laboratory, I would never be able to make this kind of plot. Therefore, I chose 200 GeV to be the defining energy difference between E_{for} and E_{back} because a difference of 200 GeV requires 20% missing energy from

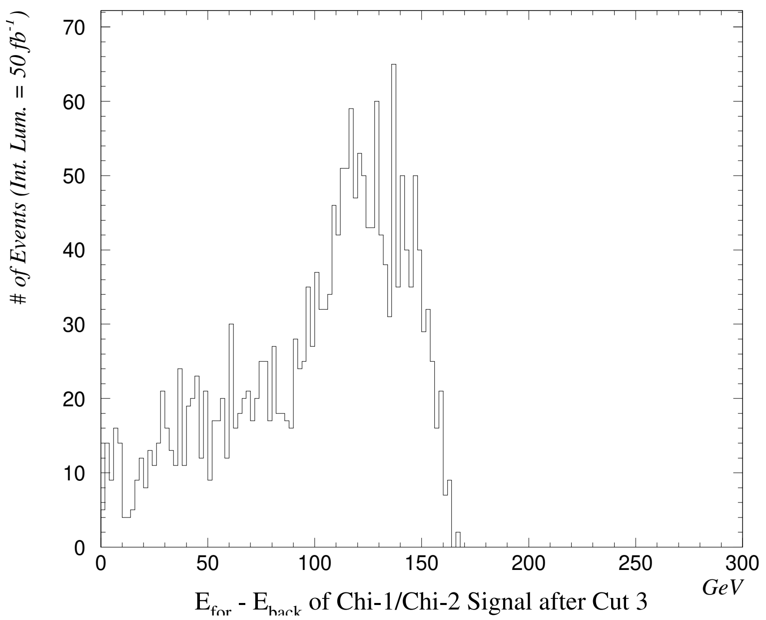

Figure 11: E$_{for}$ - E$_{back}$ of $\widetilde{\chi}_1^0\widetilde{\chi}_2^0$ signal after Cut 3.

the signal in the forward direction.

4.1.5 Cut 5

The fifth cut that I made was to require that events had no e$^+$, e$^-$, μ^+, or μ^-. This requirement was due to the fact that the neutralino signal for which I was looking had no e$^+$, e$^-$, μ^+, or μ^-. I did not want to include any events which were part of the $\widetilde{\chi}_1^0\widetilde{\chi}_2^0$ signal that had semileptonic decays. A semileptonic decay is one in which the b-quark decays into a final state that includes a lepton and a neutrino. The neutrinos present in the semileptonic decays would have given me an incorrect mass of the Higgs particle when I reconstructed the mass using the $b\bar{b}$ jets[2]. This cut removed those $\widetilde{\chi}_1^+\widetilde{\chi}_1^-$ events whose decays form e^+, e^-, μ^+, and μ^-. See Figure 12 for a Feynman diagram depicting the process by which the $\widetilde{\chi}_1^+\widetilde{\chi}_1^-$ signal is produced at an occurrance of 14.7% for each lepton (this percentage represents the branching

[2]I did not cut τ^+ or τ^-, as the Higgs can decay into τ pairs. Further, τs cannot be detected by themselves; only their decay products (most usually e^+, e^-, μ^+, or μ^- with other particles) can be detected.

ratio of this particular decay). This signal is the one which is most affected by this cut.

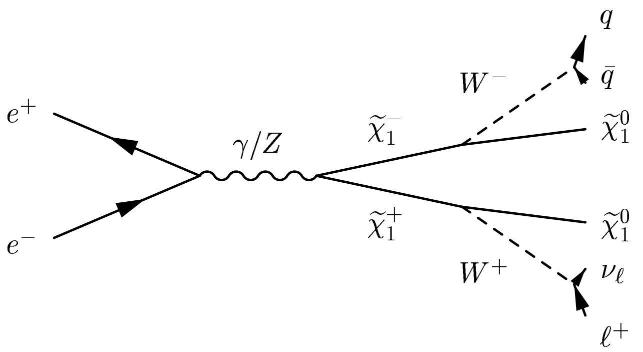

Figure 12: Feynman diagram showing one way of how the $\widetilde{\chi}_1^+\widetilde{\chi}_1^-$ signal is produced. Note that due to the symmetry of this signal, leptons with the opposite sign have an equal chance of occurring.

4.1.6 Cut 6

Finally, I cut all events that did not contain two b-quark jets. This cut was used because the Higgs is mainly coupled to b mesons. I needed to reconstruct the mass of the $b\bar{b}$ quark jets. Upon reconstructing the mass, I realized that the mass of the Higgs (from which the $b\bar{b}$ jets had decayed) was too close to that of the W particle (namely, 80.4 GeV), which was a decay product of the $\widetilde{\chi}_1^+\widetilde{\chi}_1^-$ signal. Note the $\widetilde{\chi}_1^+\widetilde{\chi}_1^-$ signal of Figure 13, which shows a branching ratio that occurs 46.1%. Figure 14 shows the two combined mass plots. These plots are a reconstruction of the $b\bar{b}$ quark jets. Note that in the top plot, which shows the reconstructed Higgs mass before the 2 b-quark jet requirement, the background is quite large. After the 2 b-quark jet requirement, the background decreases dramatically.

In order to cut all events which did not contain two b-quark jets, I used a computer subroutine written by Dr. David Wagner that detected b-quark jets. This subroutine is known as a b-tagging routine or algorithm. b-tagging is the process by which jets are identified and tagged as b-mesons by their decays.

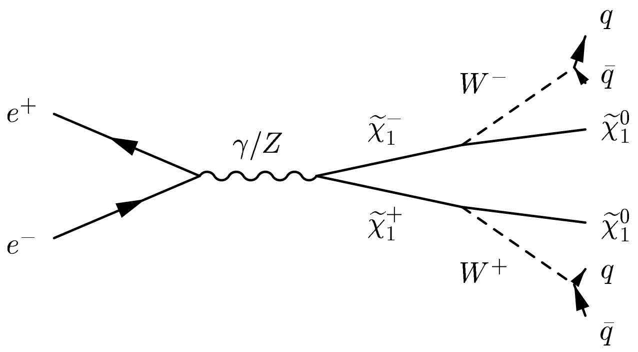

Figure 13: Feynman diagram showing one way of how the $\widetilde{\chi}_1^+\widetilde{\chi}_1^-$ signal is produced. Note that the branching ratio for this signal is 46.1%

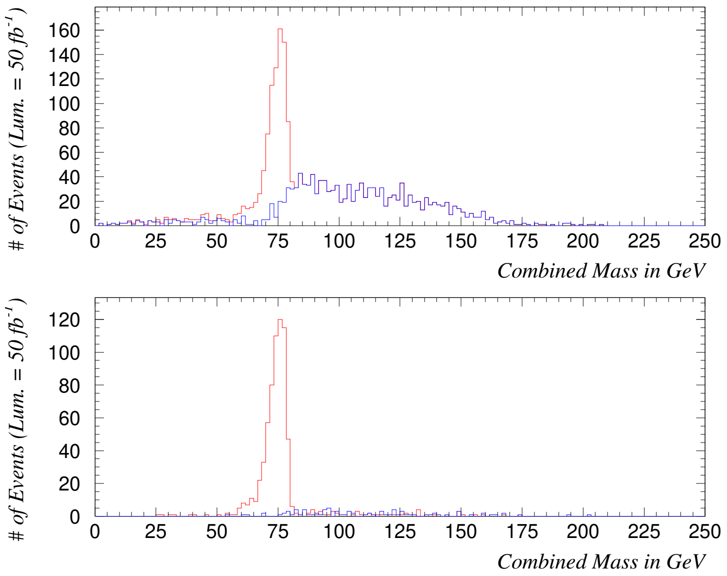

Figure 14: Reconstructed mass of the particles in the b-quark jets. In both plots, the red signal is the $\widetilde{\chi}_1^0\widetilde{\chi}_2^0$ signal plus background and the blue signal is background alone. Top plot shows the reconstructed mass before the 2 b-quark jet cut and bottom plot shows the reconstructed mass after the 2 b-quark jet cut.

While the W can decay into quark jets, it will never decay into $b\bar{b}$. It most often decays into $u\bar{d}$, $d\bar{u}$, $c\bar{s}$, or $s\bar{c}$. The problem lies in the fact that we cannot differentiate very clearly between $b\bar{b}$ and $u\bar{d}$ until we study decays near the vertex detector. By requiring events to have two b-quark jets (there was no distinguishing between a b or a $\bar{b}$ with the b-tagging routine I used), I could very effectively cut the remaining $\widetilde{\chi}_1^+\widetilde{\chi}_1^-$ signal from the background.

4.2 After the Cuts

Figure 15 shows the histogram of the visible energy of the $b\bar{b}$ system that survived the cuts. From this histogram, I made a box fit of the red signal (which is the sum of the signal plus background that survived the cuts described above).

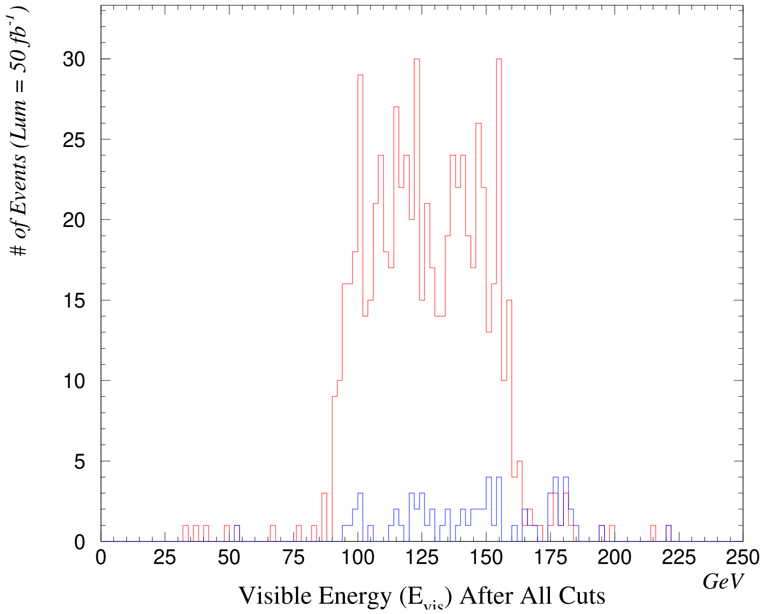

Figure 15: E_{vis} of $b\bar{b}$ system of the $\widetilde{\chi}_1^0\widetilde{\chi}_2^0$ plus background that survived the cuts (red) and E_{vis} of the Supersymmetric background alone (blue).

Figure 16 shows the box fit of the signal. The box fit shows the minimum energy (E_{min}) was 92.1 GeV, with an error of ± 1.0 GeV. The maximum energy (E_{max}) was 159.8 GeV, with an error of ± 1.1 GeV. The χ^2 for the fit was 1.05 per degree of freedom.

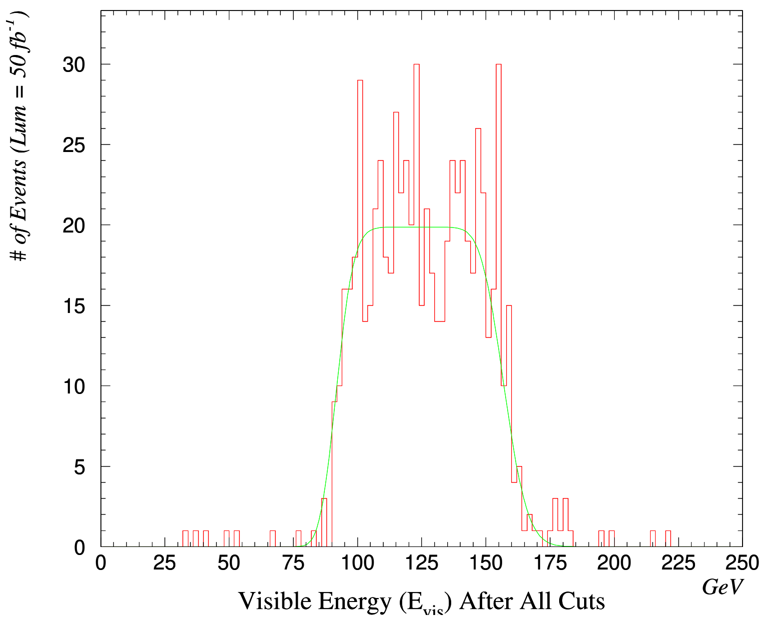

Figure 16: Box fit of the Supersymmetric signal which survived the cuts, using E_{vis} of the particles to determine the E_{min} and E_{max}.

The E_{min} and E_{max} were used to determine the masses of the $\widetilde{\chi}_1^0$ and $\widetilde{\chi}_2^0$ particles. This was done by using what is known as the Endpoint Method. In their research papers, my colleagues Nick Danielson, Liz Goodman, and Brook Williams have mathematically shown how the Endpoint Method works [6, 7, 8]. In a two-body decay, where $A \rightarrow B + C$, it is possible to determine the mass of A and B if the mass of C is known. Additionally, the center of mass energy (E_{cm}) of the reaction must be known, as well as the maximum (E_{max}) and minimum (E_{min}) energies of particle C.

Since it was required that the mass of one of the decay products be known (in this case, the mass of the Higgs), I had to reconstruct the mass of the Higgs particle from the energy and momentum of the b-quark jets. Recall that Figure 14 shows a histogram of the combined mass of the signal after all the cuts. The average of the combined mass is 82.8 GeV. I used this value as the mass of the Higgs particle. Note that it corresponds well with the expected value of 83.25 GeV (from Table 4).

I input the required values (E_{cm}, M_{higgs}, $E_{higgs,min}$, and $E_{higgs,max}$) into a program created by Nick Danielson (using the aforementioned Endpoint

Method). The values returned by the computer for the masses are shown in Table 8. These values correspond rather well with the predicted values that

Table 8: The results of my "experimentally" found masses.

Particle	Calculated Mass	Error	Theoretical Mass
$\widetilde{\chi}_1^0$	81.3 GeV	$\pm$2.0 GeV	86.05 GeV
$\widetilde{\chi}_2^0$	177.9 GeV	$\pm$1.6 GeV	175.45 GeV

were shown in Table 4, namely 86.05 GeV and 175.45 GeV. Although the discrepancies between the "experimentally" found masses and the predicted masses is larger than the error, one must keep in mind that this is only the statistical error. The systematic error is not included. Additionally, the study of the $\widetilde{\chi}_1^0\widetilde{\chi}_2^0$ signal at this point is not complete. The Standard Model background has yet to be added and then cut away.

5 Conclusion

The research I performed this summer showed that it is possible to separate the $\widetilde{\chi}_1^0\widetilde{\chi}_2^0$ signal from the other Supersymmetry signals. By performing various cuts based on branching ratios and particle decays, the $\widetilde{\chi}_1^0\widetilde{\chi}_2^0$ signal can be isolated. Once the signal is isolated, a box fit can be performed on the visible energy histogram in order to determine the high and low energy levels. It is also possible to reconstruct the mass of the Higgs particle. With the mass of the Higgs particle and the high and low energy levels, the masses of the $\widetilde{\chi}_1^0$ and $\widetilde{\chi}_2^0$ particles can be determined.

The next step is to include Standard Model background and find ways to cut it from the $\widetilde{\chi}_1^0\widetilde{\chi}_2^0$ signal. The signal will need to be isolated from it as from the Supersymmetric background. The box fit and combined mass procedures can then be performed and once again, the masses of the neutralinos can be computed.

The steps I took will be of great use in designing the Next Linear Collider's (abbreviated as NLC) detector. For instance, I used a b-tagging routine to identify b and $\bar{b}$ jets. It will be necessary to include a b-tagging device in the NLC's detector, as I have shown that in order to separate the $\widetilde{\chi}_1^0\widetilde{\chi}_2^0$ signal from the $\widetilde{\chi}_1^+\widetilde{\chi}_1^-$, we need to identify b and $\bar{b}$ quark jets. Research like this provides important feedback for the design of the detector for the Next Linear Collider.

6 Suggestions for Future Work

At this point in my research, I have been able to make a rough estimate of the masses of the $\widetilde{\chi}_1^0$ and $\widetilde{\chi}_2^0$ particles. However, my research of Point 1 is only half done. I still need to add the Standard Model background and then make cuts to remove it. After I re-compute the masses of the neutralinos, I must make a detailed error analysis of my findings, comparing them to the generating masses (those masses that are listed in Table 4).

Further work beyond that will be the isolation and measurement of other Point 1 signals. I will study other polarizations as well. Beyond that, I will study the signals of the other points. This study would greatly aid the design of the NLC's detector.

References

[1] Schwarz, Cindy, *A Tour of the Subatomic Zoo: A Guide to Particle Physics* (1992).

[2] Dodd, J. E., *The Ideas of Particle Physics: An Introduction for Scientists* (1984).

[3] Roe, B. P., *Particle Physics at the New Millenium* (1996).

[4] Haber, H.E. and Kane G.L., "The Search for Supersymmetry: Probing Physics Beyond the Standard Model," *Physics Reports* 117 (1985): 75–263.

[5] Bagger, J., *et al.*, "Summary of the Supersymmetry Working Group," *Proceedings of Snowmass '96 Conference* (1997): 642–654.

[6] Danielson, N., "Determining the Mass of the $\widetilde{\nu}_\ell$ and $\widetilde{\chi}_1^+$ By Examining the $\widetilde{\nu}_\ell\widetilde{\nu}_\ell$ Production Mode," **COLO HEP 404** (April 14, 1998).

[7] Goodman, E., "The Search for the Supersymmetric Selectron," **COLO HEP 398** (April 15, 1998).

[8] Williams, B., "Study of the Production of Supersymmetric Particles," **COLO HEP 402** (April 15, 1998).